Journal of Sound and Vibration 329 (2010) 1435–1449

Contents lists available at ScienceDirect

Journal of Sound and Vibration

journal homepage: www.elsevier.com/locate/jsvi

Polynomial versus trigonometric expansions for nonlinear vibrations of circular cylindrical shells with different boundary conditions

Ye. Kurylov [a], M. Amabili [b,*]

[a] Dipartimento di Ingegneria Industriale, Università di Parma, Viale Usberti 181/A, Parma 43100, Italy
[b] Department of Mechanical Engineering, McGill University, 817 Sherbrooke Street West, Montreal, Quebéc, Canada H3A 2K6

ARTICLE INFO

Article history:
Received 17 July 2009
Received in revised form
11 October 2009
Accepted 29 October 2009
Handling Editor: M.P. Cartmell
Available online 5 December 2009

ABSTRACT

Large-amplitude (geometrically nonlinear) forced vibrations of circular cylindrical shells with different boundary conditions are investigated. The Sanders–Koiter nonlinear shell theory, which includes in-plane inertia, is used to calculate the elastic strain energy. The shell displacements (longitudinal, circumferential and radial) are expanded by means of a double mixed series: harmonic functions for the circumferential variable and three different formulations for the longitudinal variable; these three different formulations are: (a) Chebyshev orthogonal polynomials, (b) power polynomials, and (c) trigonometric functions. The same formulation is applied to study different boundary conditions; results are presented for simply supported and clamped shells. The analysis is performed in two steps: first a liner analysis is performed to identify natural modes, which are then used in the nonlinear analysis as generalized coordinates. The Lagrangian approach is applied to obtain a system of nonlinear ordinary differential equations. Different expansions involving from 14 to 34 generalized coordinates, associated with natural modes of both simply supported and clamped–clamped shells, are used to study the convergence of the solution. The nonlinear equations of motion are studied by using arclength continuation method and bifurcation analysis. Numerical responses obtained in the spectral neighborhood of the lowest natural frequency are compared with results available in literature.

1. Introduction

A great number of studies on large-amplitude (geometrically nonlinear) vibrations of circular cylindrical shells are available; the literature published before 2003 has been reviewed by Amabili and Païdoussis [1]. The problem is also amply discussed by Amabili in his recent monograph [2]. Here the attention is focused on large-amplitude free and forced vibrations under harmonic excitation in radial direction. In the majority of the studies available, Donnell's nonlinear shallow-shell theory is applied to model the problem; see, e.g. Refs. [3–12]. However, more refined classical theories have been also used, including Donnell nonlinear shell theory retaining in-plane inertia, the Sanders–Koiter (also referred as Sanders) nonlinear shell theory, the Flügge–Lur'e–Byrne nonlinear shell theory and the Novozhilov nonlinear shell theory [9,13–23]. These theories have been compared with each other by Amabili [22]. Nonlinear shell theories retaining shear

* Corresponding author. Tel.: +1 514 398 3068; fax: +1 514 398 7365.
E-mail address: marco.amabili@mcgill.ca (M. Amabili).
URL: http://people.mcgill.ca/marco.amabili/ (M. Amabili).

0022-460X/$ - see front matter © 2009 Elsevier Ltd. All rights reserved.
doi:10.1016/j.jsv.2009.10.038

deformation and rotary inertia, developed for thick and composite laminated shells, as the first-order shear deformation and higher-order shear deformation theories have been also applied to study nonlinear vibration of circular cylindrical shells [24–28].

The literature analysis shows that several methods were developed in the past for investigating nonlinear vibrations of circular cylindrical shells with different boundary conditions. Therefore, the present study is a contribution toward developing a general framework that allows studying circular shells with different boundary conditions, comparing different expansions of mode shapes.

In the present study, large-amplitude (geometrically nonlinear) forced vibrations of circular cylindrical shells with different boundary conditions are investigated. The Sanders–Koiter nonlinear shell theory, which includes in-plane inertia, is used to calculate the elastic strain energy. The shell displacements (longitudinal, circumferential and radial) are expanded by means of a double mixed series: harmonic functions for the circumferential variable and three different formulations for the longitudinal variable; these three different formulations are: (a) Chebyshev orthogonal polynomials [29,30], (b) power polynomials, and (c) trigonometric functions. The same formulation is applied to study different boundary conditions; results are presented for simply supported and clamped shells. The analysis is performed in two steps: first a liner analysis is performed to identify natural modes, which are then used in the nonlinear analysis as generalized coordinates. The Lagrangian approach is applied to obtain a system of nonlinear ordinary differential equations. Different expansions involving from 14 to 34 generalized coordinates, associated with natural modes of both simply supported and clamped–clamped shells, are used to study the convergence of the solution. The nonlinear equations of motion are studied by using arclength continuation method and bifurcation analysis. Numerical responses obtained in the spectral neighborhood of the lowest natural frequency are compared with results available in literature.

2. Strain energy

In Fig. 1, a circular cylindrical shell having radius R, length L and thickness h is represented; a cylindrical coordinate system $(O; x, r, \theta)$ is considered in order to take advantage of the axial symmetry of the structure; the origin is placed at the center of one end of the shell. Three displacement fields are shown in Fig. 1: axial $u(x, \theta, t)$, circumferential $v(x, \theta, t)$ and radial $w(x, \theta, t)$ displacement.

Geometric imperfections can be considered in the theory by means of initial radial displacements $w_0(x, \theta)$; however, in the numerical results, only perfect shells are considered here.

The nonlinear Sanders–Koiter shell theory is used, which is a classical theory derived by using the following assumptions: (i) $h \ll R$ and $h \ll L$; (ii) the displacements are of the order of the shell thickness h; (iii) strains are small; (iv) transverse normal stresses are negligible; (v) the normal to the undeformed middle surface remains straight and normal to the middle surface after deformation, and no thickness stretching is present (Kirchhoff–Love kinematic hypothesis); and (vi) rotary inertia is neglected.

Strain components ε_x, ε_θ and $\gamma_{x\theta}$ at an arbitrary point of the shell are

$$\varepsilon_x = \varepsilon_{x,0} + zk_x, \tag{1a}$$

$$\varepsilon_\theta = \varepsilon_{\theta,0} + zk_\theta, \tag{1b}$$

$$\gamma_{x\theta} = \gamma_{x\theta,0} + zk_{x\theta} \tag{1c}$$

where z is the distance of the arbitrary point of the shell from the middle surface.

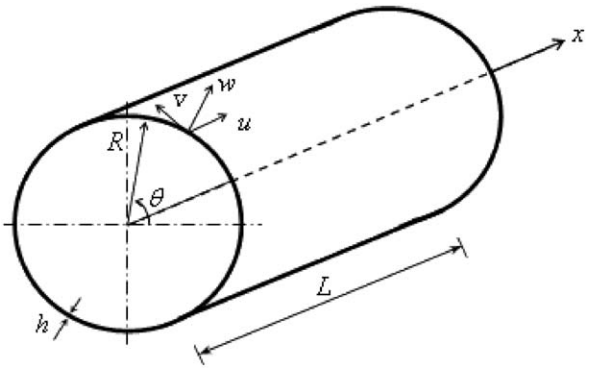

Fig. 1. Circular cylindrical shell: coordinate system and dimensions.

According to Sanders–Koiter nonlinear shell theory, the middle surface strain–displacement relationships and changes in the curvature and torsion for a circular cylindrical shell are given by [2,31–33]

$$\varepsilon_{x,0}=\frac{\partial u}{L\,\partial\eta}+\frac{1}{2}\left(\frac{\partial w}{L\,\partial\eta}\right)^2+\frac{1}{8}\left(\frac{\partial v}{L\,\partial\eta}-\frac{\partial u}{R\,\partial\theta}\right)^2+\frac{\partial w}{L\,\partial\eta}\frac{\partial w_0}{L\,\partial\eta}, \tag{2a}$$

$$\varepsilon_{\theta,0}=\frac{\partial v}{R\,\partial\theta}+\frac{w}{R}+\frac{1}{2}\left(\frac{\partial w}{R\,\partial\theta}-\frac{v}{R}\right)^2+\frac{1}{8}\left(\frac{\partial u}{R\,\partial\theta}-\frac{\partial v}{L\,\partial\eta}\right)^2+\frac{\partial w_0}{R\,\partial\theta}\left(\frac{\partial w}{R\,\partial\theta}-\frac{v}{R}\right), \tag{2b}$$

$$\gamma_{x\theta,0}=\frac{\partial u}{R\,\partial\theta}+\frac{\partial v}{L\,\partial\eta}+\frac{\partial w}{L\,\partial\eta}\left(\frac{\partial w}{R\,\partial\theta}-\frac{v}{R}\right)+\frac{\partial w_0}{L\,\partial\eta}\left(\frac{\partial w}{R\,\partial\theta}-\frac{v}{R}\right)+\frac{\partial w}{L\,\partial\eta}\frac{\partial w_0}{R\,\partial\theta}, \tag{2c}$$

$$k_x=-\frac{\partial^2 w}{L^2\,\partial\eta^2}, \tag{2d}$$

$$k_\theta=\frac{\partial v}{R^2\,\partial\theta}-\frac{\partial^2 w}{R^2\,\partial\theta^2}, \tag{2e}$$

$$k_{x\theta}=-2\frac{\partial^2 w}{LR\,\partial\eta\,\partial\theta}+\frac{1}{2R}\left(3\frac{\partial v}{L\,\partial\eta}-\frac{\partial u}{R\,\partial\theta}\right), \tag{2f}$$

where $\eta=x/L$ is the nondimensional longitudinal coordinate.

The elastic strain energy U_S of a circular cylindrical shell, neglecting σ_z as stated by in assumption (iv), is given by [2]

$$U_S=\frac{1}{2}LR\int_0^{2\pi}\int_0^1\int_{-h/2}^{h/2}(\sigma_x\varepsilon_x+\sigma_\theta\varepsilon_\theta+\tau_{x\theta}\gamma_{x\theta})\,\mathrm{d}\eta(1+z/R)\,\mathrm{d}\theta\,\mathrm{d}z, \tag{3}$$

where the stresses σ_x, σ_θ and $\tau_{x\theta}$ are related to the strains for homogeneous and isotropic material (σ_z=0, case of plane stress) by [2]

$$\sigma_x=\frac{E}{1-\nu^2}(\varepsilon_x+\nu\varepsilon_\theta), \tag{4a}$$

$$\sigma_\theta=\frac{E}{1-\nu^2}(\varepsilon_\theta+\nu\varepsilon_x), \tag{4b}$$

$$\tau_{x\theta}=\frac{E}{2(1+\nu)}\gamma_{x\theta}, \tag{4c}$$

where E is Young's modulus and ν is Poisson's ratio. By using Eqs. (1)–(3), the following expression is obtained:

$$\begin{aligned}U_S=&\frac{1}{2}\frac{Eh}{1-\nu^2}LR\int_0^{2\pi}\int_0^1\left(\varepsilon_{x,0}^2+\varepsilon_{\theta,0}^2+2\nu\varepsilon_{x,0}\varepsilon_{\theta,0}+\frac{1-\nu}{2}\gamma_{x\theta,0}^2\right)\mathrm{d}\eta\,\mathrm{d}\theta\\&+\frac{1}{2}\frac{Eh^3}{12(1-\nu^2)}LR\int_0^{2\pi}\int_0^1\left(k_x^2+k_\theta^2+2\nu k_x k_\theta+\frac{1-\nu}{2}k_{x\theta}^2\right)\mathrm{d}\eta\,\mathrm{d}\theta\\&+\frac{1}{2}\frac{Eh^3}{6R(1-\nu^2)}LR\int_0^{2\pi}\int_0^1\left(\varepsilon_{x,0}k_x+\varepsilon_{\theta,0}k_\theta+\nu\varepsilon_{x,0}k_\theta+\nu\varepsilon_{\theta,0}k_x+\frac{1-\nu}{2}\gamma_{x\theta,0}k_{x\theta}\right)\mathrm{d}\eta\,\mathrm{d}\theta+O(h^4),\end{aligned} \tag{5}$$

where $O(h^4)$ is a higher-order term in h according to the Sanders–Koiter theory. The right-hand side of Eq. (5) can be easily interpreted: the first term is the membrane (also referred as stretching) energy and the second one is the bending energy, while the last term couples the membrane and bending energies.

3. Kinetic energy, virtual work and damping

The kinetic energy T_S of a circular cylindrical shell, by neglecting rotary inertia, is given by

$$T_S=\frac{1}{2}\rho_S hLR\int_0^{2\pi}\int_0^1(\dot{u}^2+\dot{v}^2+\dot{w}^2)\,\mathrm{d}\eta\,\mathrm{d}\theta, \tag{6}$$

where ρ_s is the mass density of the shell. In Eq. (6) the overdot denotes time derivative.

The virtual work W done by the external forces is written as

$$W=LR\int_0^{2\pi}\int_0^1(q_x u+q_\theta v+q_r w)\,\mathrm{d}\eta\,\mathrm{d}\theta, \tag{7}$$

where q_x, q_θ and q_r are the distributed forces per unit area acting on the shell in axial, circumferential and radial direction, respectively.

The nonconservative damping forces are assumed to be of viscous type and are taken into account by using Rayleigh's dissipation function

$$F = \frac{1}{2} cLR \int_0^{2\pi} \int_0^1 (\dot{u}^2 + \dot{v}^2 + \dot{w}^2)\, \mathrm{d}\eta\, \mathrm{d}\theta, \tag{8a}$$

where c is the viscous damping coefficient, which has a different value for each term of the mode expansion. This viscous damping coefficient is immediately transformed into modal damping ratio.

In-plane forces and bending moments depend on the shell strains; in particular, the following relationships are useful to apply the boundary conditions:

$$M_x = \frac{Eh^3}{12(1-\nu^2)}(k_x + \nu k_\theta) = 0, \tag{9a}$$

$$N_x = \frac{Eh}{1-\nu^2}(\varepsilon_{x,0} + \nu \varepsilon_{\theta,0}) = 0. \tag{9b}$$

4. Linear vibrations: modal analysis

In order to carry out a linear vibration analysis, in the present section, linear Sanders–Koiter theory is considered, i.e. in Eq. (5), only quadratic terms are retained.

The best basis for expanding displacement fields is the eigenfunction basis, but only for special boundary conditions such basis can be found analytically; generally, eigenfunctions must be evaluated numerically.

In order to attack the general problem of circular cylindrical shell vibration, displacement fields are expanded by means of a double series: deformation in the circumferential direction is presented by harmonic functions, (a) Chebyshev polynomials are considered in the axial direction.

Let us now consider natural modes of vibration, i.e. a synchronous motion:

$$u(\eta, \theta, t) = U(\eta, \theta) f(t),$$

$$v(\eta, \theta, t) = V(\eta, \theta) f(t),$$

$$w(\eta, \theta, t) = W(\eta, \theta) f(t), \tag{10}$$

where $U(\eta, \theta)$, $V(\eta, \theta)$ and $W(\eta, \theta)$ represent the mode shape and $f(t)$ is an harmonic function.

Now the modal shape is expanded in a double series in terms of Chebyshev polynomials $T_m^*(\eta)$ and harmonic functions:

$$U(\eta, \theta) = \sum_{m=0}^{M_U} \sum_{n=0}^{N} U_{m,n} T_m^*(\eta) \cos(n\theta), \tag{11a}$$

$$V(\eta, \theta) = \sum_{m=0}^{M_V} \sum_{n=0}^{N} V_{m,n} T_m^*(\eta) \sin(n\theta), \tag{11b}$$

$$W(\eta, \theta) = \sum_{m=0}^{M_W} \sum_{n=0}^{N} W_{m,n} T_m^*(\eta) \cos(n\theta), \tag{11c}$$

where $T_m^*(\eta) = T_m(2\eta - 1)$ and $T_m(\cdot)$ is the m-th order Chebyshev polynomial of the first kind. The transformation of coordinates from η to $2\eta - 1$ is necessary since Chebyshev polynomials are defined between -1 and 1, while $T_m^*(\eta)$ has been introduced in order to be defined between 0 and 1. In Eqs. (11a–c) $U_{m,n}$, $V_{m,n}$ and $W_{m,n}$ are unknown coefficients.

For the case of (b) ordinary power polynomials instead of Eqs. (11) one will have the following expressions:

$$U(\eta, \theta) = \sum_{m=0}^{M_U} \sum_{n=0}^{N} U_{m,n} \eta^m \cos(n\theta), \tag{12a}$$

$$V(\eta, \theta) = \sum_{m=0}^{M_V} \sum_{n=0}^{N} V_{m,n} \eta^m \sin(n\theta), \tag{12b}$$

$$W(\eta, \theta) = \sum_{m=0}^{M_W} \sum_{n=0}^{N} W_{m,n} \eta^m \cos(n\theta). \tag{12c}$$

For the case of (c) trigonometric functions, one will have different expansions according to the boundary conditions. For simply supported boundary conditions the expansion is [22]

$$U(\eta,\theta)=\sum_{m=1}^{M_U}\sum_{n=0}^{N}U_{m,n}\cos(m\pi\eta)\cos(n\theta), \tag{13a}$$

$$V(\eta,\theta)=\sum_{m=1}^{M_V}\sum_{n=0}^{N}V_{m,n}\sin(m\pi\eta)\sin(n\theta), \tag{13b}$$

$$W(\eta,\theta)=\sum_{m=1}^{M_W}\sum_{n=0}^{N}W_{m,n}\sin(m\pi\eta)\cos(n\theta). \tag{13c}$$

For clamped boundary conditions, the expansions of u, v and w are given by Amabili [9].

4.1. Boundary conditions

The way to satisfy boundary conditions for expansions involving only trigonometric functions is explained e.g. in Refs. [9] and [22]. In case of polynomials, boundary conditions are satisfied by applying constraints to the unknown coefficients in expansions (11) or (12). Some of the coefficients $U_{m,n}$, $V_{m,n}$ and $W_{m,n}$ can be suitably chosen in order to satisfy boundary conditions.

For the simply supported shell the following boundary conditions are imposed:

$$w=0,\quad v=0,\quad M_x=0,\quad N_x=0 \text{ at } \eta=0,1. \tag{14a −d}$$

Initially, the expansion with Chebyshev polynomial is investigated. Eqs. (14a,b) give

$$W(\eta,\theta)=\sum_{m=0}^{M_W}\sum_{n=0}^{N}W_{m,n}T_m^*(\eta)\cos(n\theta)=0 \quad \text{for } \eta=0,1, \tag{15a}$$

$$V(\eta,\theta)=\sum_{m=0}^{M_V}\sum_{n=0}^{N}V_{m,n}T_m^*(\eta)\sin(n\theta)=0 \quad \text{for } \eta=0,1. \tag{15b}$$

Then, by using Eqs. (15a,b), Eqs. (14c,d) are reduced to

$$\frac{\partial^2 W(\eta,\theta)}{\partial\eta^2}=\sum_{m=0}^{M_W}\sum_{n=0}^{N}W_{m,n}\frac{\partial^2 T_m^*(\eta)}{\partial\eta^2}\cos(n\theta)=0 \quad \text{for } \eta=0,1, \tag{15c}$$

$$\frac{\partial U(\eta,\theta)}{\partial\eta}=\sum_{m=0}^{M_U}\sum_{n=0}^{N}U_{m,n}\frac{\partial T_m^*(\eta)}{\partial\eta}\cos(n\theta)=0 \quad \text{for } \eta=0,1. \tag{15d}$$

In Eq. (15d) nonlinear terms have been neglected. In fact, since the Rayleigh–Ritz method is used to find the solution, just geometric boundary condition has to be exactly satisfied.

Such conditions are valid for any θ and n, therefore Eqs. (15a–d) are modified as follows:

$$\sum_{m=0}^{M_W}W_{m,n}T_m^*(\eta)=0,\qquad \sum_{m=0}^{M_V}V_{m,n}T_m^*(\eta)=0,$$

$$\sum_{m=0}^{M_W}W_{m,n}\frac{\partial^2 T_m^*(\eta)}{\partial\eta^2}=0,\qquad \sum_{m=0}^{M_U}U_{m,n}\frac{\partial T_m^*(\eta)}{\partial\eta}=0,\qquad \text{for } n=0,1,\ldots \text{ at } \eta=0,1. \tag{16}$$

For the expansion using power polynomials, the boundary conditions are satisfied in a similar way. Specifically, for power polynomials equations (14a–d) become

$$\sum_{m=0}^{M_W}W_{m,n}\eta^m=0,\qquad \sum_{m=0}^{M_V}V_{m,n}\eta^m=0,$$

$$\sum_{m=0}^{M_W}W_{m,n}\frac{\partial^2(\eta^m)}{\partial\eta^2}=0,\qquad \sum_{m=0}^{M_U}U_{m,n}\frac{\partial(\eta^m)}{\partial\eta}=0,\qquad \text{for } n=0,1,\ldots \text{ at } \eta=0,1. \tag{17}$$

The linear algebraic system (16) or (17) is solved in terms of the coefficients $U_{1,n}, U_{2,n}, V_{0,n}, V_{1,n}, W_{0,n}, W_{1,n}, W_{2,n}, W_{3,n}$ for $n=0,1,\ldots$. Therefore the expansions of u, v and w can be obtained in terms of remaining unknown coefficients.

For the clamped–clamped shell, the following boundary conditions are imposed:

$$w=0, \quad \frac{\partial w}{\partial \eta}=0, \quad v=0, \quad u=0, \quad \text{at } \eta=0,1. \tag{18}$$

The procedure is formally the same as for simply supported boundary conditions; however, the resulting linear system is solved in terms of the following coefficients $U_{0,n}, U_{1,n}, V_{0,n}, V_{1,n}, W_{0,n}, W_{1,n}, W_{2,n}, W_{3,n}$ for $n=0,1,\ldots$.

4.2. Eigenvalue problem

Eqs. (10) and (11) or (12) are inserted into the expressions of kinetic and potential energies; in particular, the nonlinear terms are neglected in the potential energy. Then a set of ordinary differential equations is obtained by using the Lagrange equations. These equations can be immediately decoupled in the variable θ.

An intermediate step is the reordering of variables. A vector $\mathbf{q}$ containing all variables is built; this vector has a different structure according to the shell boundary conditions [23]. Specifically, for simply supported edges:

$$\mathbf{q}=(U_{0,0}, U_{3,0}, \ldots, U_{0,1}, U_{3,1}, \ldots, V_{2,0}, V_{3,0}, \ldots, V_{2,1}, V_{3,1}, \ldots, W_{4,0}, W_{5,0}, \ldots, W_{4,1}, W_{5,1}, \ldots)f(t). \tag{19}$$

For clamped–clamped edges:

$$\mathbf{q}=(U_{2,0}, U_{3,0}, \ldots, U_{2,1}, U_{3,1}, \ldots, V_{2,0}, V_{3,0}, \ldots, V_{2,1}, V_{3,1}, \ldots, W_{4,0}, W_{5,0}, \ldots, W_{4,1}, W_{5,1}, \ldots)f(t). \tag{20}$$

The number of variables needed to describe a mode with n nodal diameters is $M_T=M_U+M_V+M_W-5$.

Lagrange equations for free vibrations are

$$\frac{\mathrm{d}}{\mathrm{d}t}\left(\frac{\partial L}{\partial \dot{q}_i}\right)-\frac{\partial L}{\partial q_i}=0, \quad i=1,2,\ldots,N_{\max}, \tag{21}$$

where $L=T_s-U_s$ and $N_{\max}=M_T(N+1)$. Assuming harmonic motion, $f(t)=\mathrm{e}^{\mathrm{j}\omega t}$, one obtains

$$(-\omega^2\mathbf{M}+\mathbf{K})\mathbf{q}=\mathbf{0}, \tag{22}$$

which is the classical eigenvalue problem in nonstandard form; it gives natural frequencies and mode shapes.

The mode shape corresponding to the j-th mode is given by Eqs. (11) or (12), where $U_{m,n}$, $V_{m,n}$, $W_{m,n}$ are substituted with $U^{(j)}_{m,n}$, $V^{(j)}_{m,n}$, $W^{(j)}_{m,n}$, which are the components of the j-th eigenvector obtained from Eq. (22) and the vector function $\mathbf{U}^{(j)}(\eta)=(U^{(j)}(\eta), V^{(j)}(\eta), W^{(j)}(\eta))^{\mathrm{T}}$ is the j-th eigenfunction vector of the original problem.

Mode shapes are normalized by $U^{(j)}(\eta)/\max(U^{(j)}(\eta))$, $V^{(j)}(\eta)/\max(V^{(j)}(\eta))$ and $W^{(j)}(\eta)/\max(W^{(j)}(\eta))$ for any η.

One should mention that for accurate numerical calculations, a very high numerical accuracy is required in calculating the eigenvectors (mode shapes) and all the coefficients to be introduced in the matrices.

5. Nonlinear vibrations

In the nonlinear analysis, the full nonlinear expression of the potential shell energy (5), containing terms up to fourth order, is considered. Displacement fields $u(\eta,\theta,t)$, $v(\eta,\theta,t)$ and $w(\eta,\theta,t)$ are expanded by using the linear mode shapes obtained in the previous linear analysis:

$$\begin{aligned}
u(\eta,\theta,t)&=\sum_{j=1}^{M}\sum_{n=0}^{N}U^{(j)}(\eta)[u_{j,n,c}(t)\cos(n\theta)+u_{j,n,s}(t)\sin(n\theta)],\\
v(\eta,\theta,t)&=\sum_{j=1}^{M}\sum_{n=0}^{N}V^{(j)}(\eta)[v_{j,n,c}(t)\sin(n\theta)+v_{j,n,s}(t)\cos(n\theta)],\\
w(\eta,\theta,t)&=\sum_{j=1}^{M}\sum_{n=0}^{N}W^{(j)}(\eta)[w_{j,n,c}(t)\cos(n\theta)+w_{j,n,s}(t)\sin(n\theta)],
\end{aligned} \tag{23}$$

where the total number of degrees of freedom in the nonlinear analysis is $2M\times N+M$, which is generally much smaller than $N_{\max}$ used in the linear analysis. In Eqs. (23) both sin and cos mode shapes in θ are introduced since a circular cylindrical shell is axisymmetric; therefore, both families of modes are participating in the shell response.

Expansions (23) satisfy the boundary conditions and the normalized mode shapes $U^{(j)}(\eta)$, $V^{(j)}(\eta)$, $W^{(j)}(\eta)$ are known functions, evaluated in the previous linear analysis, and are expressed in terms of polynomials (except in the case of expansion with trigonometric functions, see [9,22]). In Eq. (23) the generalized coordinates $u_{j,n,c/s}(t)$, $v_{j,n,c/s}(t)$, $w_{j,n,c/s}(t)$ are obviously no more harmonic functions. Using expansion (23) one can select suitable shapes for each displacement field separately, improving convergence and reducing number of degrees of freedom. It is interesting to note that, due to the normalization, the generalized coordinates represent the maximum amplitude of vibration since $\max(U^{(j)}(\eta))$, $\max(V^{(j)}(\eta))$ and $\max(W^{(j)}(\eta))$ after normalization are one.

Expansion (23) is inserted in the expressions giving strain and kinetic energies (5) and (6), virtual work (7) and damping (8).

Only a radial harmonic concentrated force is assumed to act on the shell. The external radial distributed load q_r applied to the shell, due to the radial concentrated force $\tilde{f}$, is given by

$$q_r = \tilde{f}\,\delta(R\theta - R\tilde{\theta})\delta(x - \tilde{x})\cos(\omega t), \tag{24}$$

where ω is the excitation frequency, t is the time, δ is the Dirac delta function, $\tilde{f}$ gives the radial force amplitude positive in z direction, $\tilde{x}$ and $\tilde{\theta}$ give the axial and angular positions of the point of application of the force, respectively; here, the point excitation is assumed to be located at $\tilde{x} = L/2$, $\tilde{\theta} = 0$; as a consequence of this excitation, the generalized coordinates with subscript c are directly excited (driven modes) and those with subscript s are not directly excited (companion modes).

The following notation is introduced for brevity:

$$\mathbf{p} = \{u_{j,n,c}, u_{j,n,s}, v_{j,n,c}, v_{j,n,s}, w_{j,n,c}, w_{j,n,s}\}^{\mathrm{T}}, \quad j = 1,\ldots,M \text{ and } n = 0,\ldots,N. \tag{25}$$

The generic element of the time-dependent vector $\mathbf{p}$ is referred to as p_i; the dimension of $\mathbf{p}$ is dofs, which is the number of degrees of freedom used in the mode expansion.

The generalized forces Q_j are obtained by differentiation of Rayleigh's dissipation function and of the virtual work done by external forces

$$Q_i = -\frac{\partial F}{\partial \dot{p}_i} + \frac{\partial W}{\partial p_i}. \tag{26}$$

The Lagrange equations of motion for the shell are

$$\frac{\mathrm{d}}{\mathrm{d}t}\left(\frac{\partial T}{\partial \dot{p}_i}\right) - \frac{\partial T}{\partial p_i} + \frac{\partial U}{\partial p_i} = Q_i, \quad i = 1,\ldots \text{dofs}, \tag{27}$$

where $\partial T/\partial p_i = 0$. These second-order equations have very long expressions containing quadratic and cubic nonlinear terms.

The very complicated term giving quadratic and cubic nonlinearities can be written in the form

$$\frac{\partial U}{\partial p_i} = \sum_{k=1}^{\text{dofs}} p_k f_{k,i} + \sum_{j,k=1}^{\text{dofs}} p_j p_k f_{j,k,i} + \sum_{j,k,l=1}^{\text{dofs}} p_j p_k p_l f_{j,k,l,i}, \tag{28}$$

where coefficients f have long expressions that include also geometric imperfections.

The set of ordinary nonlinear differential equations (27) is studied by using numerical continuation methods and bifurcation analysis.

6. Numerical results

The equations of motion have been obtained by using the *Mathematica* computer software [34] in order to perform analytical surface integrals of trigonometric and Chebyshev functions. The generic Lagrange equation j is divided by the modal mass associated with $\ddot{p}_j$ and then is transformed in two first-order equations. A non-dimensionalization of variables is also performed for computational convenience: the frequencies are non-dimensionalized dividing by the natural frequency of the resonant mode and the vibration amplitudes are divided by the shell thickness h. The resulting $2 \times$ dofs equations are studied by using the software AUTO [35] for continuation and bifurcation analysis of nonlinear ordinary differential equations. The software AUTO is capable of continuation of the solution, bifurcation analysis and branch switching by using the pseudo-arclength continuation method. In particular, the shell response under harmonic excitation has been studied by using an analysis in two steps: (i) first the excitation frequency has been fixed far enough from resonance and the magnitude of the excitation has been used as bifurcation parameter; the solution has been started at zero force where the solution is the trivial undisturbed configuration of the shell and has been continued up to reach the desired force magnitude; (ii) when the desired magnitude of excitation has been reached, the solution has been continued by using the excitation frequency as bifurcation parameter.

6.1. Simply supported shell: Chebyshev polynomial versus trigonometric expansions

A test case of a simply supported circular cylindrical shell is analyzed. Calculations have been performed for a shell having the following dimensions and material properties: L=0.2 m, R=0.1 m, h=0.247 mm, E=71.02 $\times$ 10^9 Pa, ρ=2796 kg/m^3 and ν=0.31, which corresponds to a case studied by several authors [5,11,19,22,36]. The mode investigated is (m=1, n=6) which has one longitudinal half-wave and 6 circumferential waves.

Chebyshev polynomials of 15th power were used to obtain mode shapes of the problem (linear vibration study). Such high power was chosen to obtain axisymmetrical modes with relatively high number of axial half-waves m; specifically mode (m=7, n=0) and higher. But since contribution of these modes is small, in farther analysis only modes up to (5,0) are taken into consideration. Therefore polynomials of 9th power can be used to save computational time. If one has no aim to study influence of higher modes (both—axisymmetrical and asymmetrical), even polynomials of the 7th power give accurate results. Natural frequencies of some modes (important modes in the nonlinear model) obtained by using

Table 1
Comparison of natural frequencies (Hz) for simply supported shell obtained by using Chebyshev polynomials; present theory (polynomials of different power) versus exact results obtained with trigonometric functions.

Mode (m, n)	(1,n)	(1,2n)	(3,2n)	(3,n)	(1,0)
7th power Chebyshev polynomial	553.33	882.22	1439.66	3061.19	7784.15
9th power Chebyshev polynomial	553.33	882.22	1455.67	3040.78	7784.15
15th power Chebyshev polynomial	553.33	882.22	1555.56	3040.66	7784.15
Exact with trigonometric function	553.37	882.26	1455.69	3040.69	7784.15

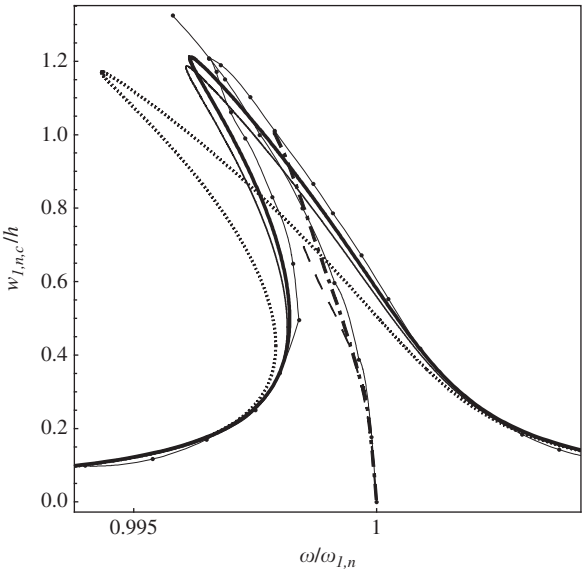

Fig. 2. Frequency–response curve for simply supported shell (only branch 1 without companion mode participation is shown). ▬▬, 28 dofs, present model with Chebyshev polynomial expansion; ——, response computed by Amabili [22]; —●—, backbone curve (free vibration) and forced response, from Pellicano et al. [11]; ····, response computed by Chen and Babcock [5]; —·—, backbone curve from Varadan et al. [34]; and — —, backbone curve from Ganapathi and Varadan [19].

polynomials of different power are compared in Table 1. The agreement is excellent (only for the 7th power polynomials, higher modes have 1 percent difference with the exact frequency).

The mode shapes for the three cases presented in Table 1 (7th, 9th and 15th power of polynomials) also perfectly coincide with the exact solution (shapes are perfect sin and cos), but, in order to obtain higher axisymmetrical modes, it is necessary to use polynomials of power 15th.

Fig. 2 shows the frequency–response curve (computed by using the model with 28 degrees of freedom) of the driven mode $w_{1,6,c}$; companion mode participation is not active. Specifically, the following modes are used in the model:

$$\begin{aligned} w:&\ (1,n),(1,2n),(1,0),(3,0),(5,0);\\ u:&\ (1,n),(1,2n),(3,2n),(1,0),(3,0),(5,0);\\ v:&\ (1,n),(1,2n),(1,3n),(1,4n),(3,2n),(3,4n). \end{aligned} \tag{29}$$

In Eq. (29) each asymmetric mode (i.e. mode with second integer number different from zero) must be counted twice to obtain the number of degrees of freedom since both cos (driven) and sin (companion) modes are used.

The present results (continuous thick line) are compared to those obtained analytically by Amabili [22], Chen and Babcock [5], Pellicano et al. [11], Ganapathi and Varadan [19] (only free vibration curve, also named backbone curve), Varadan et al. [36] (only free vibration curve). The amplitude of the external modal excitation is $\tilde{f}=0.0785\,\mathrm{N}$ and the modal damping ratio is $\zeta_{1,6}=0.0005$. The linear circular frequency of the driven and companion modes is $\omega_{1,6}=2\pi\times 553.33\,\mathrm{rad/s}$. Fig. 2 shows reasonably good agreement between the present results and those available in the literature.

In order to investigate the convergence of the expansion given in Eq. (29), the 28 dofs response is compared with reduced models; the comparison is shown in Fig. 3. Reduction of the model was performed step by step (with trials that exclude specific modes), and only the most significant cases, for which influence of the mode is high, are shown in the figure. In Fig. 3, the bold line shows the full model in Eq. (29); the dashed line represents the same model excluding mode

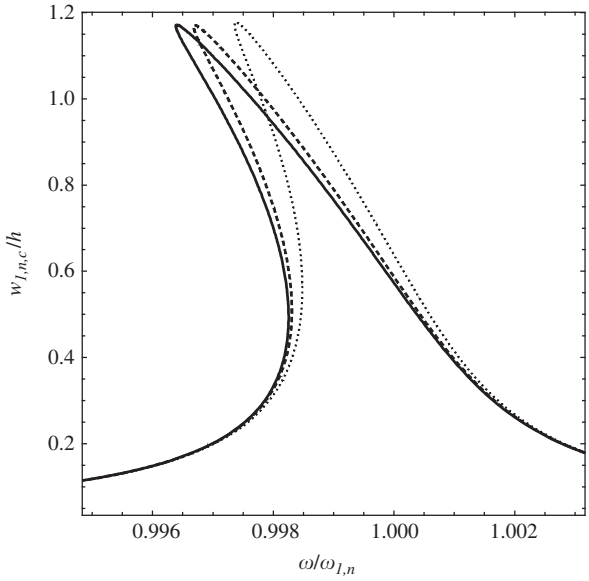

Fig. 3. Frequency–response curve for simply supported shell (only branch 1 without companion mode participation is shown). Full 28 dofs model compared to reduced models. ▬▬, 28 dofs, present model with Chebyshev polynomial expansion; — —, model excluding mode $u(3,2n)$; and ·····, model excluding $u(3,2n)$ and $v(1,3n)$.

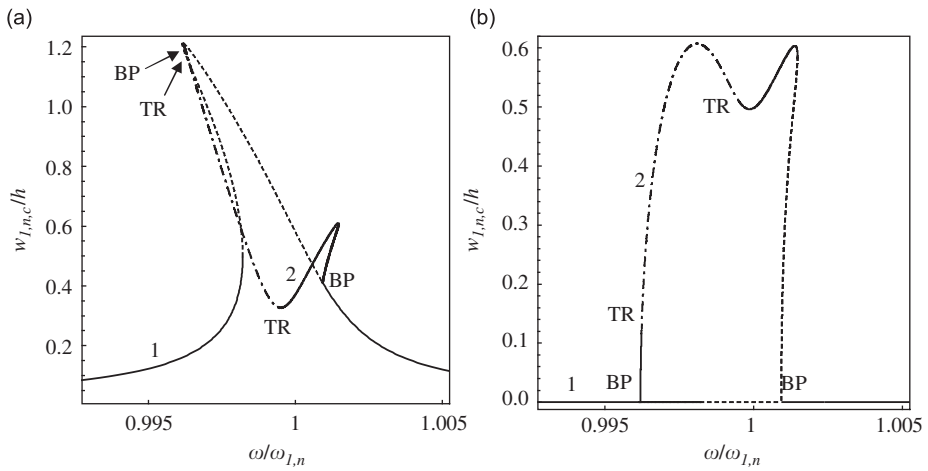

Fig. 4. Frequency–response curve for simply supported shell with companion mode participation; 28 dofs model with Chebyshev polynomial expansion. —, stable periodic solution; –·–, stable quasi-periodic solution; – –, unstable solutions; BP, pitchfork bifurcation; TR, Neimark–Sacker bifurcation; 1, branch 1; 2, branch 2. (a) Generalized coordinate $w_{1,n,c}$; and (b) generalized coordinate $w_{1,n,s}$.

$u(3,2n)$; the dotted line excludes modes $u(3,2n)$ and $v(1,3n)$. Specifically the two modes $u(3,2n)$ and $v(1,3n)$ give a contribution increasing the softening type nonlinearity, but their influence is not large; in fact, it can be expected that modes with $3n$ and $4n$ circumferential waves do not contribute significantly (the system is softening so modes with $3n$ circumferential waves play a smaller role than $2n$ modes); a similar consideration can be applied to modes with 3 axial half-waves (excluding axisymmetric modes that has to reach high axial wavenumber for convergence of the solution).

One also should note that mode having $2n$ circumferential waves $w(1,2n)$ plays a significant role in the softening behavior of the shell. The model missing that mode (not shown in the figure) shows strongly hardening behavior.

Fig. 4 shows the frequency–response relationship with companion mode participation (i.e. the actual response of the shell) for the model in Eq. (29). The main branch 1 in Fig. 4 corresponds to vibration with zero amplitude of the companion mode $w_{1,6,s}$. This branch has pitchfork bifurcations (BP) at $\omega/\omega_{1,6}=0.99619$ and at 1.00092, where branch 2 appears. This new branch corresponds to participation of both $w_{1,6,c}$ and $w_{1,6,s}$, giving a traveling-wave response moving around the shell; the phase shift between the two coordinates is almost $\pi/2$. The companion mode presents a node at the location of the excitation force and therefore it is not directly excited; its amplitude is different from zero only for large-amplitude vibrations, due to nonlinear coupling. The appearance of branch 2 is related to the 1:1 internal resonance of $w_{1,6,c}$ and $w_{1,6,s}$,

which is due to the axial symmetry of the circular cylindrical shell. This branch appears for sufficiently large excitation, and it can be observed for vibration amplitude of the order of at least 1/10 of the shell thickness.

Branch 2 undergoes two Neimark–Sacker (torus) bifurcations (TR in the figure) at $\omega/\omega_{1,6}=0.99623$ and 0.99675. Amplitude-modulated (quasi-periodic) response is indicated in Fig. 4 on branch 2 for $99623<\omega/\omega_{1,6}<0.99675$, that is, bracketed by the two Neimark–Sacker bifurcations.

6.2. Clamped shell: Chebyshev polynomial versus trigonometric expansions

Calculations have been performed for a shell having the following dimensions and material properties: $L=520$ mm, $R=149.4$ mm, $h=0.519$ mm, $E=1.98\times10^{11}$ Pa, $\rho=7800$ kg/m^3 and $\nu=0.3$. The mode investigated is ($m=1$, $n=6$).

Similarly to the case of simply supported shell, Chebyshev polynomials of 15th power have been used to obtain mode shapes. Since, as it will be shown, contribution of higher modes is significant, the power of polynomials cannot be reduced for the case of clamped shell.

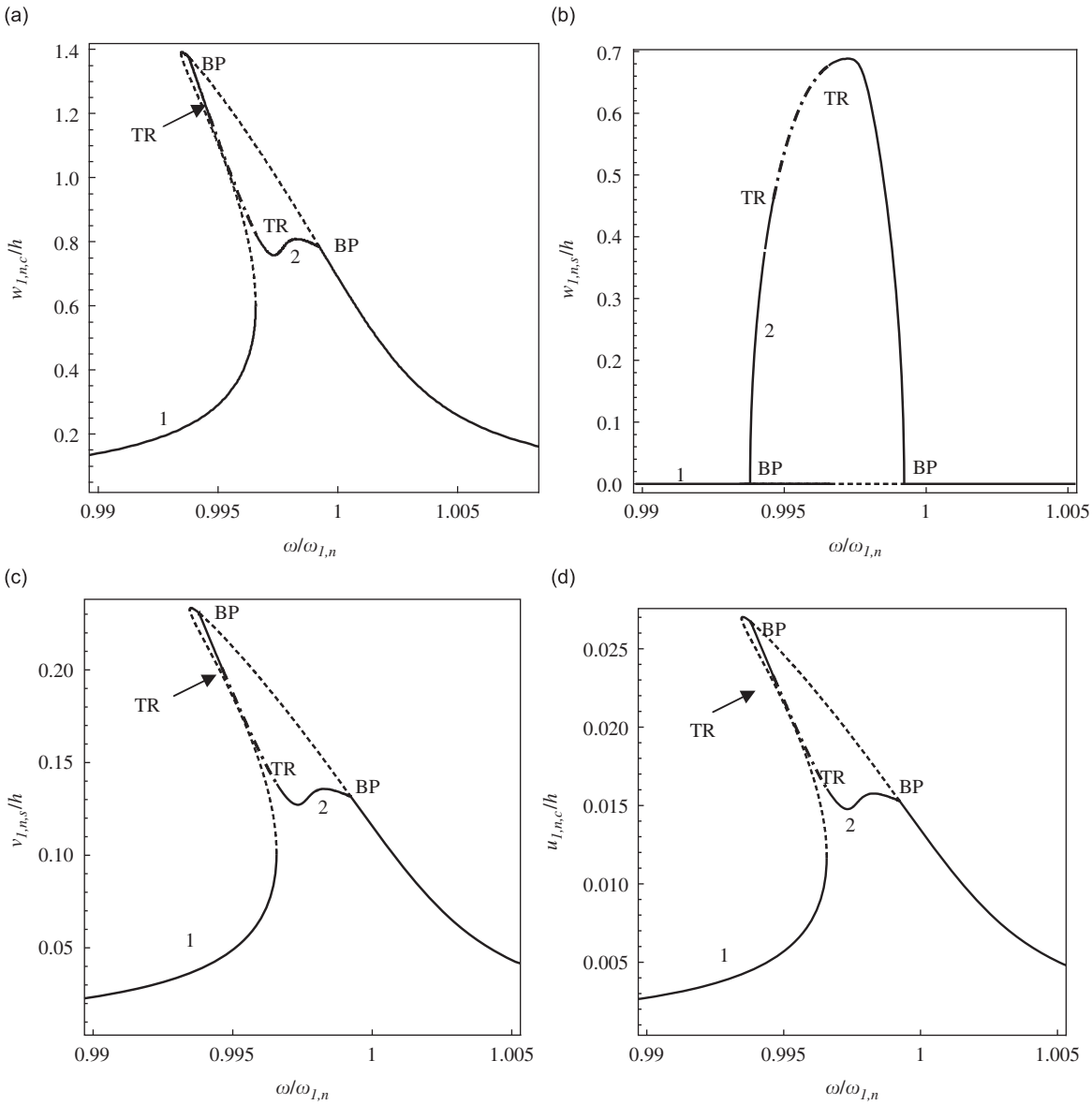

Fig. 5. Frequency–response curve for clamped shell with companion mode participation; 30 dofs model with Chebyshev polynomial expansion. —, stable periodic solution; – · –, stable quasi-periodic solution; – –, unstable solutions; BP, pitchfork bifurcation; TR, Neimark–Sacker bifurcation; 1, branch 1; 2, branch 2. (a) Generalized coordinate $w_{1,n,c}$; (b) generalized coordinate $w_{1,n,s}$; (c) generalized coordinate $v_{1,n,s}$; (d) generalized coordinate $u_{1,n,c}$; (e) generalized coordinate $w_{1,0}$; (f) generalized coordinate $u_{1,0}$; (g) generalized coordinate $w_{1,2n,c}$; and (h) generalized coordinate $w_{3,n,c}$.

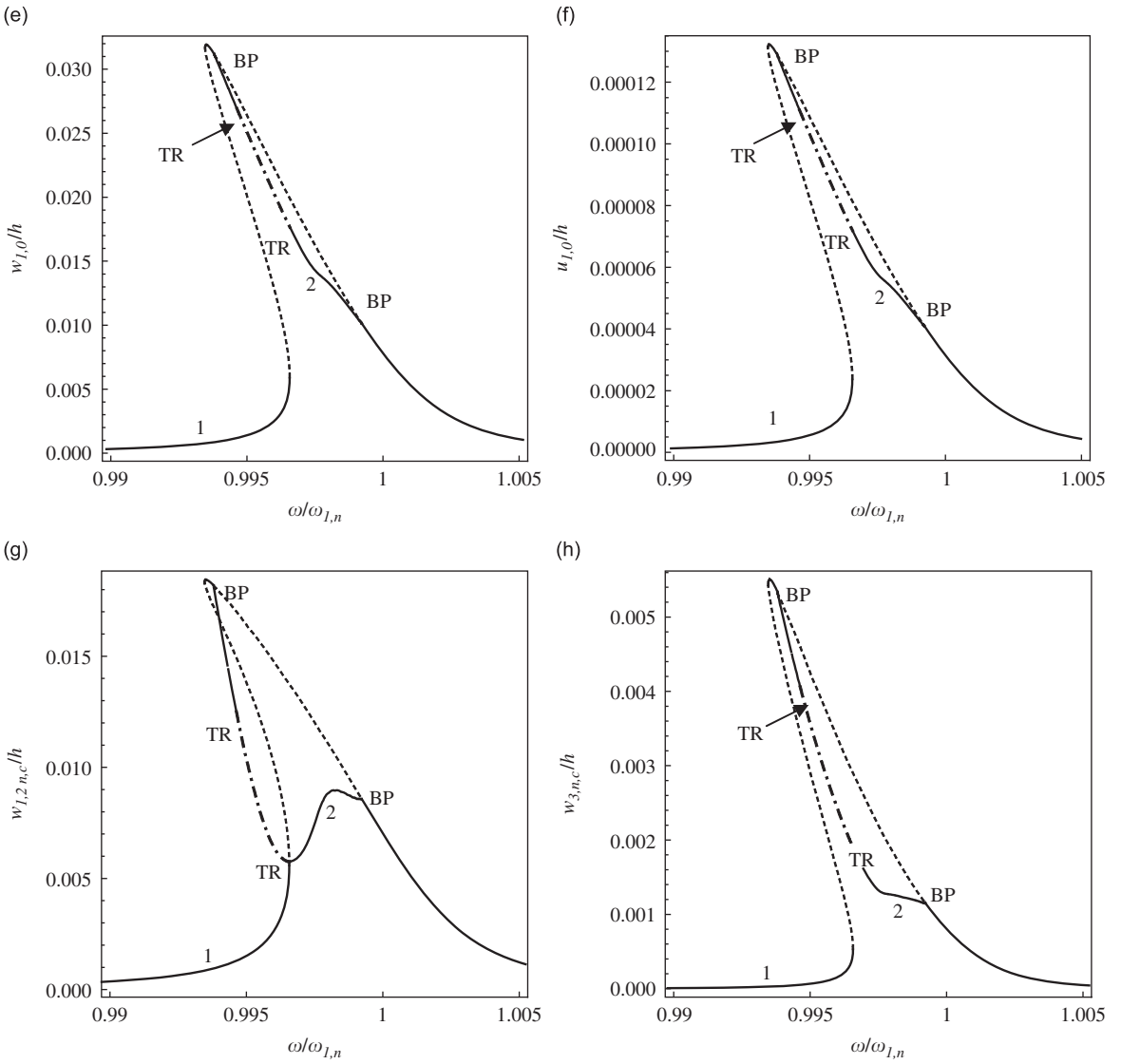

Fig. 5. (*Continued*)

The response of the circular cylindrical shell subjected to harmonic point excitation of 3 N applied at the middle of the shell in the spectral neighborhood of the lowest (fundamental) resonance $\omega_{1,n} = 2\pi \times 313.7$ rad/s, corresponding to mode (m=1, n=6), is given in Fig. 5; eight generalized coordinates are shown, just a selection of some of the most interesting coordinates, in order to show their contribution to the global response of the shell. All the calculations reported in this section, if not diversely specified, have been performed by using an expansion involving 30 generalized coordinates (with companion modes), namely:

$$w: \ (1,n),(1,2n),(3,2n),(1,0),(3,0),(5,0),(7,0),(9,0),(11,0),$$

$$u: \ (1,n),(1,2n),(3,2n),(1,0),(3,0),(5,0),(7,0),(9,0),(11,0),$$

$$v: \ (1,n),(1,2n),(3,2n). \tag{30}$$

The main coordinates in Fig. 5 are the driven and companion resonant modes, given in Figs. 5(a) and (b), respectively. The solution initially presents a single branch 1 with one folding and the typical softening type behaviour; this branch corresponds to driven mode vibration with zero amplitude of the companion mode. Branch 1 presents a pitchfork bifurcation around the peak of the response where branch 2 arises and branch 1 loses stability. Branch 2 is the solution with participation of both driven and companion modes, giving a standing wave plus a travelling wave response around the shell. Branch 2 loses stability at a Neimark–Sacker (torus) bifurcation where amplitude-modulations of the solution arise; modulations end at a second Neimark–Sacker bifurcation. Branch 2 ends at a second pitchfork bifurcation where it

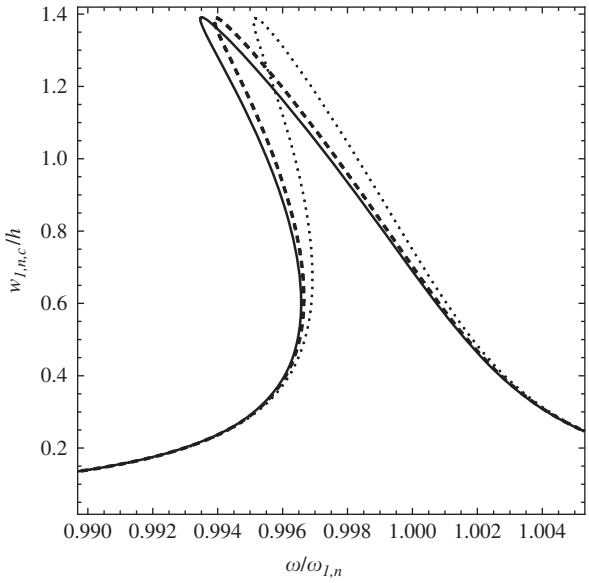

Fig. 6. Frequency–response curve for the clamped shell (without companion modes participation); full model comparing with reduced models. ▬▬, 30 dofs, present model with Chebyshev polynomial expansion; — —, model excluding modes $u(7,0)$ and $w(7,0)$; and ·····, model excluding $u(3,0)$ and $w(3,0)$.

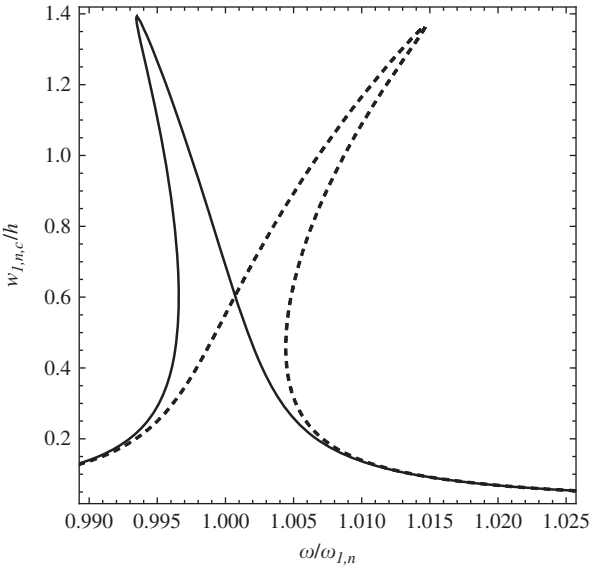

Fig. 7. Frequency–response curve for the clamped shell (without companion modes participation); full model comparing with reduced models. ▬▬, 30 dofs, present model with Chebyshev polynomial expansion; and — —, model excluding modes $u(9,0)$ and $w(9,0)$.

merges with branch 1 that regains stability. Figs. 5(c) and (d) show the response of in-plane coordinates; Figs. 5(e) and (f) present axisymmetric coordinates; finally Figs. 5(g) and (h) show the generalized coordinates $w_{1,2n,c}$ and $w_{3,n,c}$, respectively.

In order to investigate the convergence of expansion (30), the 30 dofs response is compared with reduced models; comparison is shown in Fig. 6. The bold line presents the full model given in Eq. (30), dotted line presents the same model excluding modes $u(3,0)$ and $w(3,0)$, dashed line excludes modes $u(7,0)$ and $w(7,0)$. Modes $u(5,0)$ and $w(5,0)$ have no significant effect on response of the shell (not shown in the figure). This result shows that the 30 dofs model can be reduced to the size of the simply supported model without a significant reduction of accuracy.

A farther investigation of the convergence has been performed. In fact, higher order axisymmetrical modes (namely, $u(9,0)$ and $w(9,0)$) are strictly required in expansion since absence of these modes changes the shell response from softening type to strongly hardening; this is shown in Fig. 7.

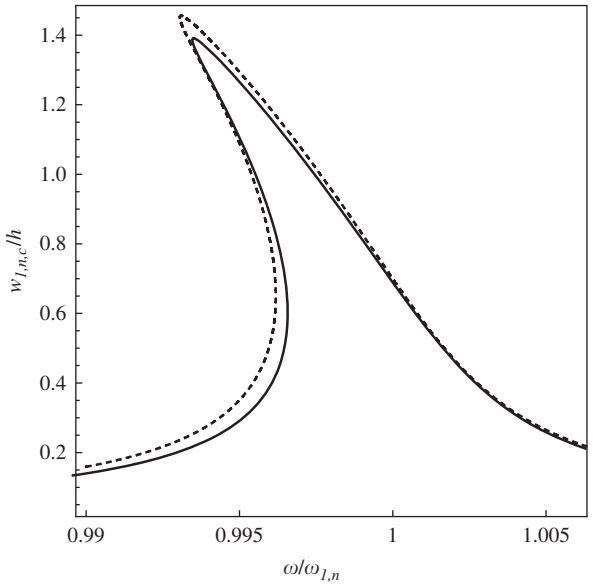

Fig. 8. Frequency-response curve for the clamped shell obtained by using Chebyshev polynomial expansions (30 dofs) compared with results obtained by Amabili [22] with trigonometric functions. ▬▬, 30 dofs, present model with Chebyshev polynomial expansion; and — —, results from Amabili [22].

Table 2
Comparison of natural frequencies (Hz) for simply supported shell obtained by using power polynomials; present theory (polynomials of different power) versus exact results obtained with trigonometric functions.

Mode (m, n)	(1,n)	(1,2n)	(3,2n)	(3,n)	(1,0)
9th power polynomial	553.33	882.22	1455.67	3040.78	7784.15
Exact with trigonometric function	553.37	882.26	1455.69	3040.69	7784.15

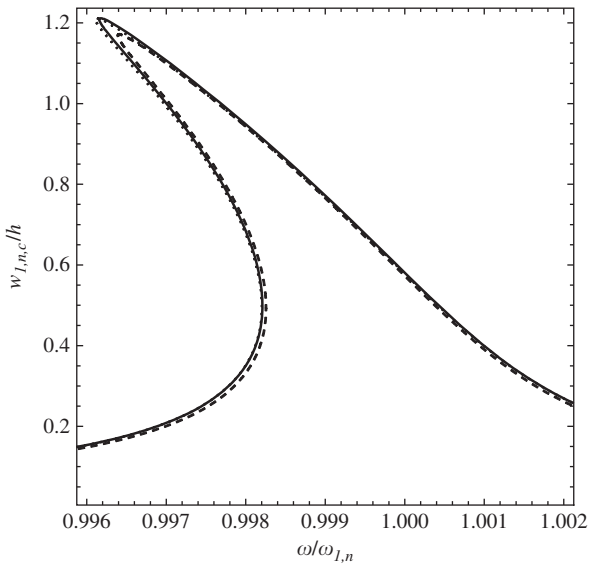

Fig. 9. Frequency–response curve for the simply supported shell obtained by using Chebyshev polynomials (▬▬, solid line), ordinary power polynomials (·····, dotted line) compared to results obtained by Amabili [22] with trigonometric functions (— —, dashed line).

The present results are also compared in Fig. 8 to those obtained by Amabili [22] using Donnell's nonlinear theory and trigonometric functions in the expansions. The agreement between these two results is quite good.

6.3. Power polynomial versus Chebyshev polynomial and trigonometric expansions for simply supported shell

The mode expansion in Eq. (29) is used for both power and Chebyshev polynomials and for trigonometric functions. To have perfect comparison, power polynomials of the same power of Chebyshev polynomials were used. Calculations show that high powers (higher than 9th power) are not applicable for ordinary power polynomials, since increasing power mass and stiffness matrixes become very badly conditioned even using extremely high precision during calculations in Mathematica [34]. Polynomials of 9th power give acceptable mode shapes (perfect sin and cos) and frequencies but do not allow considering axisymmetric modes higher than (5,0). Natural frequencies of some modes (important modes in the nonlinear model) are presented for comparison in Table 2; the agreement with the exact solution is excellent.

Fig. 9 compares the shell response for the three different types of expansions: Chebyshev polynomials, power polynomials and trigonometric functions. Results are very close each other.

7. Conclusions

The response of circular cylindrical shells with different boundary conditions has been computed by using Sanders–Koiter theory. Displacements have been expanded by means of a double series: deformation in the circumferential direction is expanded by using trigonometric functions, while Chebyshev or ordinary power polynomials are applied to expand the displacements in the axial direction.

The approach used in the present study has the advantage of being suitable for different boundary conditions, and of being very flexible to structural modifications without complication of the solution procedure. Comparison of present results with results available in literature has been carried out, showing good agreement.

A minimum mode expansion necessary to capture the nonlinear response of the shell in the neighborhood of a resonance has been determined and convergence of the solution has been numerically investigated for both simply supported and clamped shells. Models with about 20 degrees of freedom show very good convergence of results. They can be slightly reduced, but of a few units, and still presenting reasonably good results. In order to have a further reduction of the model, specific techniques can be used, as the nonlinear normal modes; otherwise the in-plane inertia has to be neglected. However, this further reduction can be paid with some loss of accuracy.

Trigonometric functions are very efficient for simply supported boundary conditions. Additional degrees of freedom are required for different boundary conditions; this decreases the computational efficiency. On the other side, Chebyshev polynomials require similar degrees of freedom for any boundary condition, representing an advantage. Finally, ordinary power polynomials present badly conditioned mass and stiffness matrices in the linear problem, so that the calculation of natural mode shapes of higher modes can become problematic.

References

[1] M. Amabili, M.P. Païdoussis, Review of studies on geometrically nonlinear vibrations and dynamics of circular cylindrical shells and panels, with and without fluid-structure interaction, *Applied Mechanics Reviews* 56 (2003) 349–381.
[2] M. Amabili, *Nonlinear Vibrations and Stability of Shells and Plates*, Cambridge University Press, New York, USA, 2008.
[3] D.A. Evensen, Nonlinear flexural vibrations of thin-walled circular cylinders, NASA TN D-4090, 1967.
[4] E.H. Dowell, C.S. Ventres, Modal equations for the nonlinear flexural vibrations of a cylindrical shell, *International Journal of Solids and Structures* 4 (1968) 975–991.
[5] J.C. Chen, C.D. Babcock, Nonlinear vibration of cylindrical shells, *AIAA Journal* 13 (1975) 868–876.
[6] V.D. Kubenko, P.S. Koval'chuk, T.S. Krasnopol'skaya, Effect of initial camber on natural nonlinear vibrations of cylindrical shells, *Soviet Applied Mechanics* 18 (1982) 34–39.
[7] M. Amabili, F. Pellicano, M.P. Païdoussis, Non-linear dynamics and stability of circular cylindrical shells containing flowing fluid. Part I: stability, *Journal of Sound and Vibration* 225 (1999) 655–699.
[8] M. Amabili, F. Pellicano, M.P. Païdoussis, Non-linear dynamics and stability of circular cylindrical shells containing flowing fluid, Part II: large-amplitude vibrations without flow, *Journal of Sound and Vibration* 228 (1999) 1103–1124.
[9] M. Amabili, Nonlinear vibrations of circular cylindrical shells with different boundary conditions, *AIAA Journal* 41 (2003) 1119–1130.
[10] A.A. Popov, J.M.T. Thompson, F.A. McRobie, Chaotic energy exchange through auto-parametric resonance in cylindrical shells, *Journal of Sound and Vibration* 248 (2001) 395–411.
[11] F. Pellicano, M. Amabili, M.P. Païdoussis, Effect of the geometry on the nonlinear vibrations analysis of circular cylindrical shells, *International Journal of Non-Linear Mechanics* 37 (2002) 1181–1198.
[12] M. Amabili, Theory and experiments for large-amplitude vibrations of empty and fluid-filled circular cylindrical shells with imperfections, *Journal of Sound and Vibration* 262 (2003) 921–975.
[13] J. Mayers, B.G. Wrenn, On the nonlinear free vibrations of thin circular cylindrical shells. Developments in Mechanics, *Proceedings of the 10th Midwestern Mechanics Conference*, Johnson Publishing Co, New York, 1967, pp. 819–846.
[14] J.H. Ginsberg, Large amplitude forced vibrations of simply supported thin cylindrical shells, *Journal of Applied Mechanics* 40 (1973) 471–477.
[15] L.J. Mente, Dynamic nonlinear response of cylindrical shells to asymmetric pressure loading, *AIAA Journal* 11 (1973) 793–800.
[16] A. Maewal, Miles' evolution equations for axisymmetric shells: simple strange attractors in structural dynamics, *International Journal of Non-Linear Mechanics* 21 (1986) 433–438.
[17] A. Maewal, Finite element analysis of steady nonlinear harmonic oscillations of axisymmetric shells, *Computer Methods in Applied Mechanics and Engineering* 58 (1986) 37–50.
[18] P.B. Gonçalves, R.C. Batista, Non-linear vibration analysis of fluid-filled cylindrical shells, *Journal of Sound and Vibration* 127 (1988) 133–143.

[19] M. Ganapathi, T.K. Varadan, Large amplitude vibrations of circular cylindrical shells, *Journal of Sound and Vibration* 192 (1996) 1–14.
[20] A. Selmane, A.A. Lakis, Influence of geometric non-linearities on free vibrations of orthotropic open cylindrical shells, *International Journal for Numerical Methods in Engineering* 40 (1997) 1115–1137.
[21] A.A. Lakis, A. Selmane, A. Toledano, Non-linear free vibration analysis of laminated orthotropic cylindrical shells, *International Journal of Mechanical Sciences* 40 (1998) 27–49.
[22] M. Amabili, Comparison of different shell theories for large-amplitude vibrations of empty and fluid-filled circular cylindrical shells with and without imperfections: Lagrangian approach, *Journal of Sound and Vibration* 264 (2003) 1091–1125.
[23] F. Pellicano, Vibrations of circular cylindrical shells: theory and experiments, *Journal of Sound and Vibration* 303 (2007) 154–170.
[24] J.N. Reddy, K. Chandrashekhara, Geometrically non-linear transient analysis of laminated, doubly curved shells, *International Journal of Non-Linear Mechanics* 20 (1985) 79–90.
[25] Y. Kobayashi, A.W. Leissa, Large-amplitude free vibration of thick shallow shells supported by shear diaphragms, *International Journal of Non-Linear Mechanics* 30 (1995) 57–66.
[26] C. Sansour, P. Wriggers, J. Sansour, Nonlinear dynamics of shells: theory, finite element formulation, and integration schemes, *Nonlinear Dynamics* 13 (1997) 279–305.
[27] C. Sansour, W. Wagner, P. Wriggers, J. Sansour, An energy–momentum integration scheme and enhanced strain finite elements for the non-linear dynamics of shells, *International Journal of Non-Linear Mechanics* 37 (2002) 951–966.
[28] M. Amabili, J.N. Reddy, R.A. Arciniega, A new nonlinear higher-order shear deformation theory for large-amplitude vibrations of laminated doubly curved shells, International Journal of Non-Linear Mechanics, submitted for publication.
[29] D. Zhou, Y.K. Cheung, S.H. Lo, F.T.K. Au, 3D vibration analysis of solid and hollow circular cylinders via Chebyshev–Ritz method, *Computer Methods in Applied Mechanics and Engineering* 192 (2003) 1575–1589.
[30] K.P. Soldatos, A. Messina, Vibration studies of cross-ply laminated shear deformable circular cylinders on the basis of orthogonal polynomials, *Journal of Sound and Vibration* 218 (2) (1998) 219–243.
[31] N. Yamaki, *Elastic Stability of Circular Cylindrical Shells*, North-Holland, Amsterdam, 1984.
[32] J.L. Sanders Jr., Nonlinear theories for thin shells, *Quarterly of Applied Mathematics* 21 (1963) 21–36.
[33] W.T. Koiter, On the nonlinear theory of thin elastic shells. I, II, III, *Proceedings Koninklijke Nederlandse Akademie van Wetenschappen B* 69 (1966) 1–54.
[34] S. Wolfram, *The Mathematica Book*, fourth ed., Cambridge University Press, Cambridge, UK, 1999.
[35] E.J. Doedel, A.R. Champneys, T.F. Fairgrieve, Y.A. Kuznetsov, B. Sandstede, X. Wang, *AUTO 97: Continuation and Bifurcation Software for Ordinary Differential Equations (with HomCont)*, Concordia University, Montreal, Canada, 1998.
[36] T.K. Varadan, G. Prathap, H.V. Ramani, Non-linear free flexural vibration of thin circular cylindrical shells, *American Institute of Aeronautics and Astronautics Journal* 27 (1989) 1303–1304.